Role of tungsten oxide in inverted polymer solar cells

Chen Tao, Shengping Ruan, Guohua Xie, Xiangzi Kong, Liang Shen, Fanxu Meng, Caixia Liu, Xindong Zhang, Wei Dong,[a] and Weiyou Chen
State Key Laboratory on Integrated Optoelectronics, College of Electronic Science and Engineering, Jilin University, 2699 Qianjin Street, Changchun 130012, People's Republic of China

(Received 5 December 2008; accepted 8 January 2009; published online 29 January 2009)

Tungsten oxide (WO_3) was inserted as an anode interfacial layer between the photoactive layer and top electrode in inverted polymer solar cells (PSCs) with nanocrystalline titanium dioxide as an electron selective layer. The device with WO_3 exhibited a remarkable improvement in power conversion efficiency compared with that without WO_3, which indicated that WO_3 efficiently prevented the recombination of charge carriers at the organic/top electrode interface. The dependence of the device performances on WO_3 film thickness and different top metal electrodes was investigated. Transparent inverted PSCs with thermally evaporable Ag/WO_3 as a transparent anode were also investigated when introducing a WO_3 buffer layer. © *2009 American Institute of Physics*. [DOI: 10.1063/1.3076134]

Interest in solar cells to capture sunlight and generate electricity is increasing due to oil energy crisis and rising concerns over global climate change. Inorganic solar cells can yield high power conversion efficiency but the expensive fabrication process makes them infeasible in common use. Instead, polymer solar cells (PSCs) are a good candidate because semiconducting polymers can be dissolved in common solvents and printed like inks so that economical roll-in-roll fabrication process can be realized.[1,2] The photoactive layer composed of electron donating and accepting materials absorbs light and generates excitons. Then electrons and holes can be efficiently separated from each other due to the nanometer-scale interpenetrating network of electron donor and acceptor within the whole photoactive layer.[3] However, a simple structure that sandwiched the photoactive layer between two electrodes (anode and cathode) is not perfect enough. The low efficiency of charge collection at the interface between the photoactive layer and electrodes results in poor performance of PSCs.[4] In order to solve this problem, interfacial layers, such as a combination of poly(3,4-ethylenedioxythiophene):poly(styrenesulfonate) (PEDOT:PSS) and lithium fluoride (LiF), are commonly introduced between the active layer and electrodes to improve charge carrier collection and to enhance the open-circuit voltage (V_{oc}).[5]

Nevertheless, PEDOT:PSS has been demonstrated to have a side effect on the performance of PSCs due to its corrosion to indium tin oxide (ITO) and electrical inhomogeneities.[6–8] In order to overcome this problem, one might simply introduce interfacial layer materials to improve the performance of PSCs. Recently, molybdenum oxide (MoO_3), vanadium oxide (V_2O_5), and nickel oxide (NiO) have been demonstrated to effectively substitute PEDOT:PSS as the anodic buffer layer in PSCs.[9,10] An alternative approach is to reverse the device architecture and hence to form inverted PSCs, in which MoO_3 and V_2O_5 were usually inserted between the active layer and top electrode.[11,12] In this letter, we introduce a low-cost, nontoxic, and easily evaporable tungsten oxide (WO_3) as a hole-extraction layer in inverted PSCs with nanocrystalline titanium dioxide (nc-TiO_2) as an electron selective layer. The device architecture is shown schematically in Fig. 1(a), and the energy level diagrams of different materials used in the device fabrication are shown in Fig. 1(b). Meanwhile, transparent inverted PSCs are fabricated with thermally evaporable Ag(13 nm)/WO_3(40 nm) as a transparent anode when introducing a 10 nm WO_3 buffer layer.

Detailed processes of preparing TiO_2-sol have been described in our previous paper.[12] After a cleaning step, TiO_2-sol was spin coated on ITO-coated glass substrates at 3000 rpm. Then the samples were moved to a muffle furnace and annealed at 450 °C for 2 h. After annealing treatment,

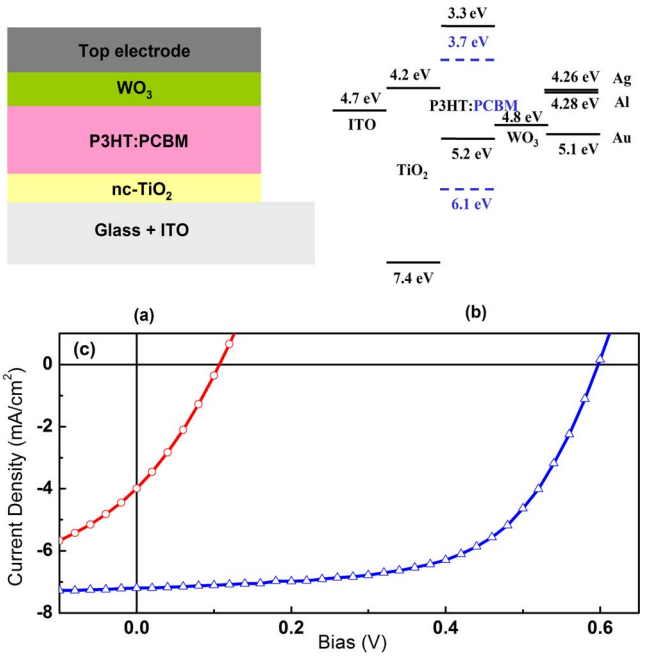

FIG. 1. (Color online) (a) The device structure of the inverted PSCs. (b) Scheme of the energy levels of the materials involved in the inverted PSCs. (c) The *J-V* characteristics of the devices under 100 mW/cm^2 white light illumination in air: ITO/nc-TiO_2/P3HT:PCBM/Ag (circle) and ITO/nc-TiO_2/P3HT:PCBM/WO_3(10 nm)/Ag (triangle).

[a]Author to whom correspondence should be addressed. Electronic mail: taochen-1984@163.com.

nc-TiO_2 was formed. In this letter, poly(3-hexylthiophene) (P3HT) (Rieke Metals) was used as electron donor material, and 6,6-phenyl C_{61} butyric acid methyl ester (PCBM) (Solenne BV) was used as electron acceptor material. The mixed chlorobenzene solution composing of P3HT (10 mg/ml) and PCBM (8 mg/ml) was then spin coated on top of the nc-TiO_2 layer at 700 rpm in ambient air. Then the samples were heated in low vacuum (vacuum oven) at approximately 150 °C for 10 min. Subsequently, the samples were pumped down in vacuum ($<10^{-3}$ Pa). Finally WO_3 and 60 nm top electrode (Ag, Au, and Al) were thermally evaporated in sequence. The active area of the device was about 0.064 cm^2.

Current density-voltage (*J-V*) characteristics of the devices were measured by a computer-controlled Keithley 2601 source meter in air without any encapsulation. The light source is a 500 W xenon lamp (CHF-XM-500W, Beijing Changtuo). The light intensity was calibrated with a Si photodetector (FZ-A, Photoelectric Instrument Factory of Beijing Normal University).

Figure 1(c) shows the current density-voltage (*J-V*) characteristics of the device with and without WO_3 under 100 mW/cm^2 white light illumination. In the absence of WO_3, the simple device (ITO/nc-TiO_2/P3HT:PCBM/Ag) exhibits a power conversion efficiency of 0.13% with a very low fill factor (FF) of 30.4%. The short-current density (J_{sc}) and V_{oc} are 3.99 mA/cm^2 and 0.107 V, respectively. However, by introducing a 10 nm WO_3 layer between the active layer and Ag, the device exhibits a power conversion efficiency of 2.58% with J_{sc}=7.20 mA/cm^2, V_{oc}=0.597 V, and FF=60.0%.

By inserting a 10 nm WO_3 buffer layer, the device (ITO/nc-TiO_2/P3HT:PCBM/WO_3/Ag) gives rise to a significant increase in J_{sc} from 3.99 to 7.20 mA/cm^2. This indicates that WO_3 efficiently prevents the recombination of charge carriers at the organic/Ag interface. Considering the device without WO_3, both P3HT and PCBM are in direct contact with Ag. It is possible for PCBM to transfer electrons to Ag electrode, thereby increasing the recombination rate of photogenerated charges. However, inserting a WO_3 layer will introduce two additional interfaces (P3HT:PCBM/WO_3 and WO_3/Ag). The high work function of WO_3 (−4.8 eV) (Ref. 4) will enhance hole collection at the photoactive layer/Ag interface.

It is known that the bulk resistance of the active materials and the contact resistance contribute to the series resistance. The contact resistance originates from the interface between the photoactive layer and electrodes. The series resistance, defined by the slope of the *J-V* curve at J=0 mA/cm^2, is estimated to be ~15.2 and ~20.0 Ω cm^2 for the devices with and without WO_3, respectively. Although most of the carriers are generated in the photoactive layer, their collection is relative to the contact resistance at the organic/top electrode interface.[13] The decrease in series resistance indicates that the insertion of the thin WO_3 film suppresses the contact resistance remarkably.

It is observable that the device without WO_3 exhibits a very low V_{oc} of 0.107 V, which is a main factor for the low power conversion efficiency. However, by incorporating a WO_3 interfacial layer, the V_{oc} has an obvious improvement and reaches up to 0.597 V. This might be caused by the increased built-in potential when introducing a WO_3 interfacial layer, for the V_{oc} is the voltage where the applied bias equals the built-in potential in an ideal diode.

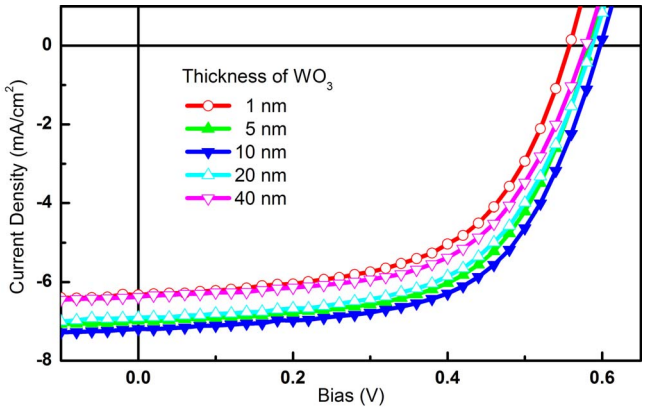

FIG. 2. (Color online) The *J-V* characteristics under 100 mW/cm^2 white light illumination in air for devices with different thickness of WO_3 used as the buffer layer between the active layer and Ag electrode.

Similar to J_{sc} and V_{oc}, the FF also increases remarkably from 30.4% to 60.0% due to the incorporation of WO_3, leading to a significant improvement in power conversion efficiency. The decrease in series resistance from 20.0 to 15.2 Ω cm^2 contributes partly to the increase in FF. Meanwhile, the shunt resistance, defined by the slope of the *J-V* curves near 0 V under illumination, is estimated to be ~1200.4 and ~39.6 Ω cm^2 for the devices with and without WO_3, respectively. The elevated shunt resistance also makes contribution to the improvement in FF.

It is necessary for the WO_3 interfacial layer to cover the active layer fully and uniformly to reduce the leakage current. However, introducing a WO_3 layer will generally contribute to the series resistance of the device and the higher thickness of WO_3 will result in a lower current. Therefore, the effect of WO_3 film thickness on device performance is investigated and shown in Fig. 2. The detailed result is summarized in Table I. The optimum thickness of WO_3 is 5–10 nm. When the thickness of WO_3 is 1 nm or less, the active layer will not be fully covered by WO_3, which tends to form some small islands instead of a uniform film. Thereafter, two additional interfaces (polymer/Ag and polymer/WO_3/Ag) are introduced. The *J-V* curve of the device with 1 nm WO_3 can be regarded as the overlapping of two independent *J-V* curves of the devices with Ag and WO_3/Ag as top electrode, respectively.[9] Due to the bad performance of the simple device (ITO/nc-TiO_2/P3HT:PCBM/Ag), the overlapping of the two independent *J-V* curves will result in a worse performance than that of a device with WO_3/Ag.

Figure 3 shows the device performance dependences on different top metal electrodes (Ag, Au, and Al) when the

TABLE I. Short-circuit current density (J_{sc}), open-circuit voltage (V_{oc}), FF, and power conversion efficiency (PCE) of inverted PSCs dependent on the thickness of WO_3.

WO_3 (nm)	J_{sc} (mA/cm^2)	V_{oc} (V)	FF (%)	PCE (%)
1	6.33	0.557	57.3	2.02
5	6.99	0.584	60.0	2.45
10	7.20	0.597	60.0	2.58
20	6.91	0.586	58.5	2.37
40	6.38	0.578	58.6	2.16

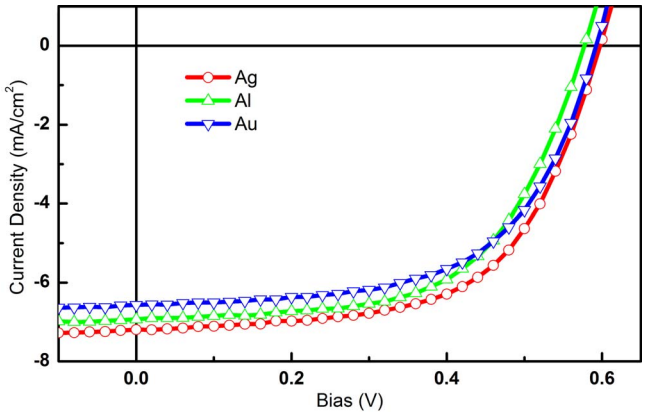

FIG. 3. (Color online) The *J-V* characteristics under 100 mW/cm^2 white light illumination in air for devices with different top metal electrodes (Ag, Au, and Al).

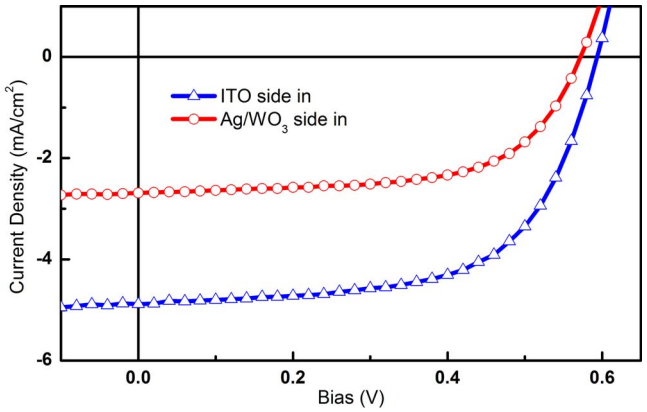

FIG. 4. (Color online) The *J-V* characteristics under 100 mW/cm^2 white light illumination in air for transparent inverted polymer solar cells illuminated from two transparent electrodes-ITO and Ag/WO_3.

thickness of WO_3 is 10 nm. Au devices exhibit a power conversion efficiency of 2.31% with J_{sc} of 6.57 mA/cm^2 and V_{oc} of 0.592 V. Al devices exhibit a power conversion efficiency of 2.37% with J_{sc} of 6.93 mA/cm^2 and V_{oc} of 0.577 V. Compared with Ag devices, Au devices show a lower efficiency because of the small absorption of incident light by Au electrode.[14] Since the test of *J-V* characteristics is carried out in ambient air, the oxidization of Al results in a larger series resistance, which induces a slightly lower efficiency in Al devices. However, devices with different top electrodes have a V_{oc} of ~0.59 V with a variation of 20 mV, which indicates that the V_{oc} is relatively irrespective of the choice of top metal electrodes when introducing a 10 nm WO_3 interfacial layer.

Recently, a WO_3/Ag/WO_3 electrode structure has been demonstrated to have a high transparency and a low sheet resistance in organic light emitting diodes due to an optical effect in the WO_3/Ag/WO_3 structure and the low resistance of the Ag layer, respectively.[15] Considering the device structure with Ag as top electrode mentioned above, it is easy to realize transparent inverted PSCs with a device structure of ITO/nc-TiO_2/P3HT:PCBM/WO_3(10 nm)/Ag(13 nm)/ $\times WO_3$(40 nm). The 10 nm WO_3 layer here is used as a buffer layer. Both ITO and Ag/WO_3 are highly transparent. The *J-V* curves for this transparent inverted PSC are shown in Fig. 4 when illuminated from ITO or Ag/WO_3 side. The device shows a power conversion efficiency of 1.80% with J_{sc} of 4.89 mA/cm^2 and V_{oc} of 0.592 V when illuminated from ITO side. However, the power conversion of the device is 0.96% with J_{sc} of 2.69 mA/cm^2 and V_{oc} of 0.572 V when illuminated from Ag/WO_3 side. The difference in power conversion efficiency is attributed to the different transparency between ITO and Ag/WO_3. Compared with the device with a reflected top electrode, the light absorption in the photoactive layer is less in transparent inverted PSC and hence to result in a lower power conversion efficiency.

In summary, we have explored the use of WO_3 in inverted polymer solar cells. Due to the high work function (−4.8 eV), WO_3 efficiently extracts holes and suppresses electrons from the active layer. The thicknesses of WO_3 and different top metal electrodes on device performances are also investigated. Transparent inverted PSCs are fabricated with Ag(13 nm)/WO_3(40 nm) as a transparent top electrode when introducing a 10 nm WO_3 buffer layer, which have the potential to realize a multiple device structure to absorb more solar photons by the multiple photoactive layers to achieve high device performance.

The authors are grateful to Major Project of Science and Technology Development Plan of Jilin Provincial Science and Technology Department (Grant Nos. 20070402 and 20080330) and the National Natural Science Foundation of China (Grant No. 60877041) for the support in the work.

[1] H. Hoppe and N. S. Sariciftci, J. Mater. Res. **19**, 1924 (2004).
[2] S. E. Shaheen, D. S. Ginley, and G. E. Jabbour, MRS Bull. **30**, 10 (2005).
[3] G. Yu, J. Gao, J. C. Hummelen, F. Wudl, and A. J. Heeger, Science **270**, 1789 (1995).
[4] M. Y. Chan, C. S. Lee, S. L. Lai, M. K. Fung, F. L. Wong, H. Y. Sun, K. M. Lau, and S. T. Lee, J. Appl. Phys. **100**, 094506 (2006).
[5] M. Reyes-Reyes, K. Kim, and D. L. Carroll, Appl. Phys. Lett. **87**, 083506 (2005).
[6] Y.-H. Kim, S.-H. Lee, J. Noh, and S.-H. Han, Thin Solid Films **510**, 305 (2006).
[7] M. P. de Jong, L. J. van Ijzendoorn, and M. J. A. de Voigt, Appl. Phys. Lett. **77**, 2255 (2000).
[8] C. Ionescu-Zanetti, A. Mechler, S. A. Carter, and R. Lal, Adv. Mater. (Weinheim, Ger.) **16**, 385 (2004).
[9] V. Shrotriya, G. Li, Y. Yao, C. Chu, and Y. Yang, Appl. Phys. Lett. **88**, 073508 (2006).
[10] M. D. Irwin, D. B. Buchholz, A. W. Hains, R. P. H. Chang, and T. J. Marks, Proc. Natl. Acad. Sci. U.S.A. **105**, 2783 (2008).
[11] G. Li, C.-W. Chu, V. Shrotriya, J. Huang, and Y. Yang, Appl. Phys. Lett. **88**, 253503 (2006).
[12] C. Tao, S. Ruan, X. Zhang, G. Xie, L. Shen, X. Kong, W. Dong, C. Liu, and W. Chen, Appl. Phys. Lett. **93**, 193307 (2008).
[13] C. Lin, S. Tseng, Y. Liu, Y. Tai, S. Chattopadhyay, C. Lin, J. Lee, J. Hwang, Y. Hsu, L. Chen, W. Chen, and K. Chen, Appl. Phys. Lett. **92**, 233302 (2008).
[14] C. Waldauf, M. Morana, P. Denk, P. Schilinsky, K. Coakley, S. A. Choulis, and C. J. Brabec, Appl. Phys. Lett. **89**, 233517 (2006).
[15] S. Y. Ryu, J. H. Noh, B. H. Hwang, C. S. Kim, S. J. Jo, J. T. Kim, H. S. Hwang, H. K. Baik, H. S. Jeong, C. H. Lee, S. Y. Song, S. H. Choi, and S. Y. Park, Appl. Phys. Lett. **92**, 023306 (2008).